



Research Article

Longshore sediment transport: predicting rates in dissipative sandy beaches at southern Brazil



Gabrielle Pereira Quadrado¹  · Elaine Siqueira Goulart² 

Received: 6 March 2020 / Accepted: 17 July 2020 / Published online: 25 July 2020
© Springer Nature Switzerland AG 2020

Abstract

Longshore sediment transport (LST) acts on beach morphodynamics on distinct temporal scales, being fundamental over sediment budget, and, so over the dynamic balance of coastlines. This study determined the most adequate methodology to estimate rates of non-cohesive sediments (from fine sand to gravel) transported by longshore currents, in the surf zone, under different meteoceanographic conditions, at the southern coast of Rio Grande do Sul (RS), Brazil. The methods proposed by CERC (Shore Protection Manual, Coastal Engineering Research Center (CERC), US Army Corps of Engineers Research and Development Center, Coastal and Hydraulics Laboratory, Vicksburg, 1984), Kamphuis (J Waterw Port Coast Ocean Eng 117(6):624–640, 1991), Bayram *et al.* (Coast Eng 54:700–710, 2007) and Van Rijn (Coast Eng 90:23–33, 2014) were tested through the comparison with data collected with streamer traps, as well as through statistical tests. Van Rijn (2014) was elected the most suitable approach for all beaches studied, followed by CERC (1984). The other two did not perform well for the study area. All models resulted in underestimated rates during high-energy scenarios, and this is attributed to wind negligence or insufficient weight factor in model's calculations, besides the lack of sampled data during very energetic conditions. Wave characteristics, median grain size and beach slope were proven to strongly influence LST, in accordance with the choice of best model overall. LST behavioural response and model's effectiveness will be different for each specific region, especially in what concerns the beach morphodynamic stage. Hence, the method prediction accuracy depends greatly on the suitability of the dataset with respect to the analytical model being used.

Keywords Sediment transport · Analytical model · Wave climate · Longshore current · Littoral drift

1 Introduction

Coastal zones represent interface areas between the continents and the oceans, where a significant part of the global population settles given their logistic, recreational and cultural potentials, and the availability of resources. Sandy beaches are coastal environments that vary in time and space accordingly to the depositional morphology and the hydrodynamic behaviour of the region in which they are located [1]. The gradients generated by hydrodynamic processes cause alterations in beach morphology

at the same time as the acting hydrodynamic is altered accordingly to the changes induced by morphology. Given the dynamics of coastal processes, sediments are constantly being moved; therefore, they are one of the most important morphodynamic components of these beaches. Hence, the sediment budget of a system modulates the dynamic balance of the coastline in different spatial and temporal scales [2].

Longshore currents (LC) are generated by the oblique incidence of waves on the coast and flow parallel to this interface, besides having potential to transport sediments

✉ Gabrielle Pereira Quadrado, gabriellepquadrado@gmail.com | ¹Programa de Pós-Graduação em Geociências (PPGGEO), Instituto de Geociências (IGEO) – Universidade Federal do Rio Grande do Sul - UFRGS, Av. Bento Gonçalves, Prédio 43113, Porto Alegre, RS 91501-970, Brazil. ²Laboratório de Oceanografia Geológica (LOG), Instituto de Oceanografia (IO) - Universidade Federal Do Rio Grande - FURG, Av. Itália, km 8, s/n, Bairro Carreiros, Rio Grande, RS 96203-000, Brazil.



by suspended load or bedload, constituting, thus, the longshore sediment transport (LST) [3]. LST acts on beach morphodynamics in temporal scales from short to long term [4], playing a fundamental role on sediment budget, mainly in microtidal regions dominated by wave action [5]. The disturbance of this budget can be triggered by natural phenomena or by anthropic interference, and persistent LST gradients, even in low rates, can result in impacts like coastline retreat [3, 4].

The prediction of LST rates and its effects are the aim of many studies developed in oceanography and coastal engineering fields [4, 6–15]. Yet, there is no consistent agreement of which is the best methodology to make predictions. Numerical modelling (process-based and analytical) is one of the most used methods when it comes to estimate LST rates, considering the limitations imposed by the adversities of measuring it in situ due to the surf zone hydrodynamics. Furthermore, numerical models represent a systematic comprehension of longshore transport once they allow the integration and the insertion of many parameters involved in this mechanism [2, 14].

Mixed beaches are composed of both sand and gravel fractions and are commonly distributed along the shorelines worldwide [16]. Given their complex dynamic associated with sorted grains of multiple sizes, the LST mechanism of mixed beaches is historically less investigated, and so, poorly understood when compared to the progress already made towards sandy beaches [16–21]. LST rates of beaches with coarser grain sizes and steeper slopes result from a different balance of morphodynamic processes than environments with fine sand; thus, classic formulae proposed, initially, for sandy beaches may not be suitable for mixed and shingle beaches [20]. In recent years, there is a growing interest concerning the establishment of reliable methods to predict LST rates in these beaches. New formulae have been proposed, and older analytical models have been revalidated and/or calibrated [4, 16, 20–23].

Hence, this study proposed the investigation and validation of the most applicable methodology to estimate the longshore transport of non-cohesive sediments at the southern shore of Rio Grande do Sul, Brazil, along varying grain size beaches. The potential of classic analytical models was evaluated like CERC [24] and Kamphuis [25], as well as two more recent alternatives developed by Bayram et al. [26] and Van Rijn [23]. All consist of analytical formulae considering process-based models in their creation and calibration processes. In this manner, the best alternative considering the study area was identified.

Mil-Homens et al. [4] and Van Rijn [23] also compared the efficiency of the models investigated herein [23–25], finding underestimated rates for energetic meteoceanographic conditions and overestimated values for low energy scenarios, for all the methods evaluated. When the

parameters considered in the equation of each of these three models are compared, many similarities occur, specially between [23, 25]. Van Rijn [23] derives from an older formula proposed in Van Rijn [22], in which the new equation was obtained from a trial with CERC [24], Kamphuis [25] and a process-based model. The same parameters considered in [25] were maintained, because these studies found a good response of LST rates to profile shape/beach slope, significant wave height and median grain size. However, weight factors were modified and Van Rijn [23] also added low-period swell, wind and tide effects.

Overall, this research is a cooperation with previous studies, which also examined the LST mechanism in different regions around the world [4, 5, 12–15, 20, 21, 23], aiming the advancement of more accurate longshore transport assessing tools, thus contributing to the comprehension of short-term coastline evolution, the evaluation of sediment budgets for coastal areas and the long-term stability of beach protection measures [23].

2 Physical settings

The study was conducted at the southern shore of Rio Grande do Sul (RS), Brazil, considering the region located between Mar Grosso Beach, to the north of Patos Lagoon mouth in São José do Norte city, and Concheiros Beach, in Santa Vitória do Palmar city (Fig. 1). Field work made in this research was carried out in Cassino Beach, Rio Grande. The other field datasets in this study were obtained by Perotto [27] and Fontoura et al. [2] in the following places: Cassino beach, the roots of the jetties in Patos Lagoon, Mar Grosso beach, Sarita, Verga, Albardão, Concheiros and Concheiros Sul.

The southern shore of RS is approximately 220 km long, oriented by a NE–SW axis, with an almost straight coastline with subtle wavy stretches. It is characterized by a wide adjacent continental shelf, with a varying slope (smoother to the north, next to Cassino beach, and steeper to the south, close to Albardão and Concheiros).

Cassino is a dissipative beach, presenting intermediate stages with troughs, alongshore rhythmic bars and rip currents [28–31]. Concheiros Beach has reflective characteristics; thus, it is more susceptible to wave action and erosion [28]. The remaining beaches are under intermediate morphodynamic stages, displaying variations along the coast. The diversity is, partially, due to beach slope and the varying grain size distribution. The coast is predominantly composed of fine sand from Mar Grosso Beach until the north of Sarita lighthouse, influenced by Patos Lagoon discharge. The occurrence of thicker grain sizes, such as coarse sand and biotrititic gravel, is more common to the south of the study area, from Albardão lighthouse to

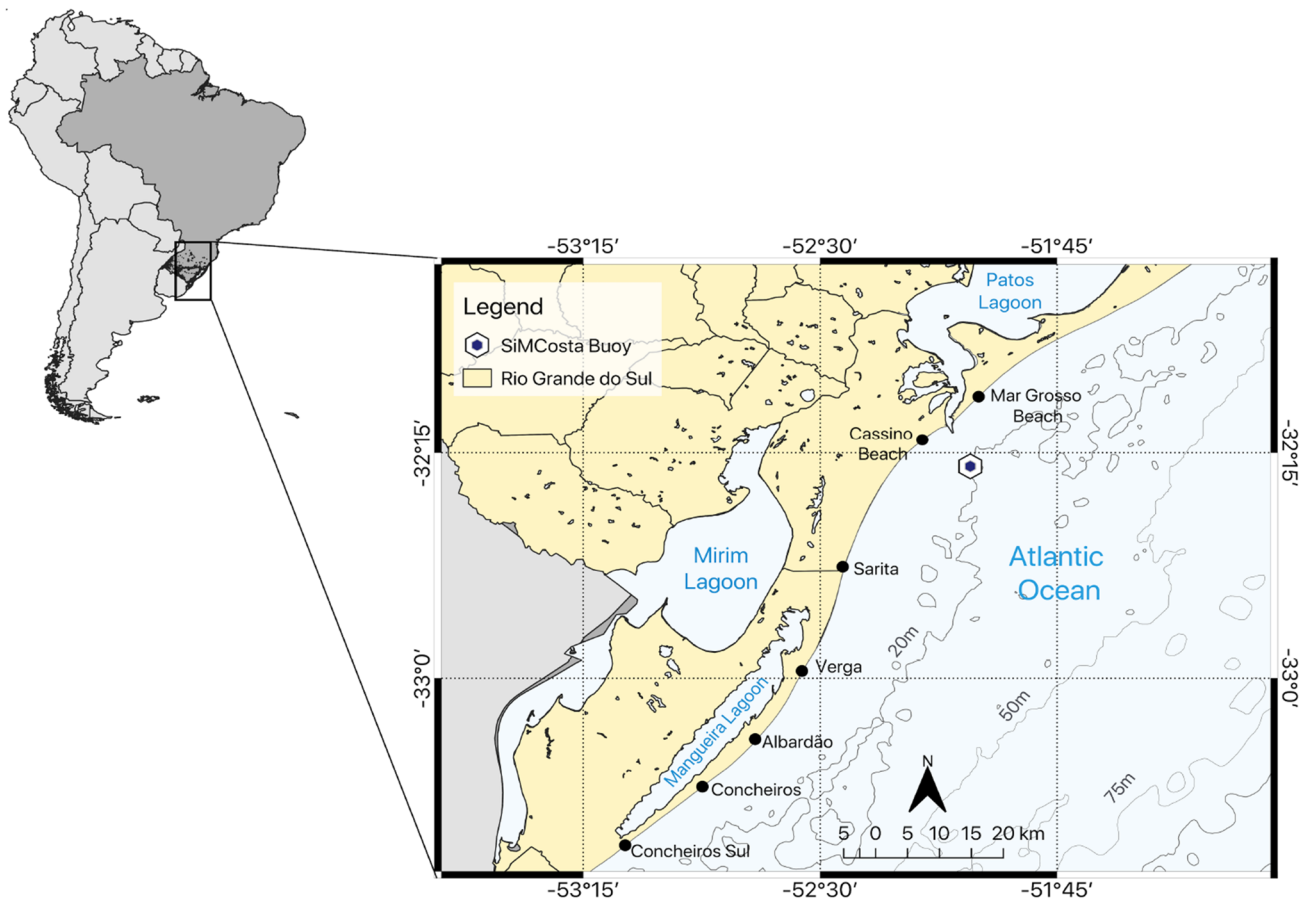


Fig. 1 Map of the study area, in which black dots represent the sampling sites of field surveys and the hexagon corresponds to the SiMCosta buoy

Concheiros Beach [28, 32]. Beach declivity increases from Mar Grosso (≈ 0.018) towards Concheiros (≈ 0.077). More details regarding grain size and beach slope data of each site under study are given in Table 1 of Sect. 3.3.

The astronomical tide follows a microtidal semidiurnal regime [36]. However, the meteorological tide can reach levels around 1.90 m during the occurrence of high-energy events [36, 37]. Two high-pressure systems of winds influence the RS coast: the South Atlantic anticyclone and the migratory polar anticyclones. The dominant wind throughout the whole year comes from NE, but the alternation among these two systems makes NE winds more frequent during spring and summer (September to February) and winds coming from the south quadrant more often through fall and winter (April to August), concomitantly with the incidence of frontal systems and the passage of storms [36, 38].

Wave climate is the most important hydrodynamic agent in this area, and it is characterized by three types of waves: swell, sea waves and storm waves [36]. Swell waves are originated mainly from SE by the tempestuous

subpolar belt in the South Atlantic, sea waves usually propagate from NE, generated by the local winds, and storm waves are less frequent, but represent the most energetic ones. Littoral drift is bidirectional along the whole state, with a net transport towards NE associated with the intensification of littoral drift and LST during the passage of storms and highly energetic events [36–41].

3 Material and methods

3.1 Field surveys

Field surveys were similar for all the author's mentioned herein, with a few differences regarding wind and wave data collection. The samples of non-cohesive sediments transported by longshore currents were collected with streamer traps developed by Kraus [9], installed in the surf zone. The trap is a metallic structure, 1.80 m high, and it displays a set of 10 capture nets (nylon, 63 μm mesh). The nets are numbered from 1 to 10, bottom to top, and

Table 1 Values of physical–chemical parameters and beach morphology data used in the analytical models

Parameter	Symbol	Value	References
Porosity	ϕ	0.3739	Author's measurement
Particle settling velocity	W_s	0.0181 m s ⁻¹ (EMA—Cassino)	Espírito Santo [33]
		0.0210 m s ⁻¹ (Mar Grosso)	
		0.0125 m s ⁻¹ (Terminal/West Jetty—Cassino)	Calliari et al. [28]
		0.0181 m s ⁻¹ (Sarita)	
		0.0181 m s ⁻¹ (Verga)	
		0.0204 m s ⁻¹ (Albardão)	
Gravity acceleration	g	0.0220/0.1500 m s ⁻¹ (Concheiros/Concheiros Sul) ^a	
		9.80665 m s ⁻²	–
Dimensionless coefficient	K	0.01	CERC [24] modified by Fontoura et al. [2]
Median grain size	D_{50}	0.125 mm (EMA—Cassino)	Author's measurement
		0.136 mm (Terminal/West Jetty—Cassino)	Fontoura et al. [2]
		0.144 mm (Mar Grosso)	Figueiredo and Calliari [29]
		0.177 mm (Sarita)	Calliari et al. [28]
		0.177 mm (Verga)	
		0.192 mm (Albardão)	
Beach slope	$\tan \beta$	0.210/0.707 mm (Concheiros/Concheiros Sul) ^a	
		0.022 (EMA—Cassino)	Author's measurement
		0.020 (Terminal—Cassino)	Fontoura et al. [2]
		0.0185 (West Jetty—Cassino)	
		0.0180 (Mar Grosso—East Jetty)	
		0.0140 (Mar Grosso—3 km)	
		0.0225 (Mar Grosso—12 km)	
		0.056 (Sarita)	Calliari et al. [28]
Sediment density	ρ_s	0.043 (Verga)	
		0.053 (Albardão)	
Seawater density	ρ_{H_2O}	0.077 (Concheiros/Concheiros Sul)	
		2650 kg m ⁻³	Martins [34]
Wind-induced longshore current velocity	$V_{LC\ WIND}$	1025 kg m ⁻³	Bessler and Rodrigues [35]
Swell factor	K_{swell}	1.0 for $T_p < 9\ s, H_s < 0.7\ m$ (absent swell)	Author's measurement
		1.5 for $T_p \geq 9\ s, H_s \geq 0.7\ m$ (swell) ^b	Van Rijn [23]

^aConcheiros presents a bimodal sediment distribution, in which fine sand is represented by $D_{50}=0.2102\ mm$ and $W_s=0.0220\ m\ s^{-1}$, and the bioterritic gravel is denoted by $D_{50}=0.707\ mm$ and $W_s=0.1500\ m\ s^{-1}$

^b K_{swell} is based on the percentage of low-period swell wave heights of the total wave height record = p_{swell} . Considering wave data used herein regards the exact period in which in situ surveys were conducted, $p_{swell}=100\%$

have different lengths: 1 to 6 = 60 cm, 7 to 8 = 70 cm and 9 to 10 = 110 cm. The size variation aims to optimize operational efficiency according to considerations made in [2, 9].

Samples were collected during a 3–5-min interval, since after this period bottom flow is altered due to the presence of the trap, misrepresenting, thus, its natural dynamic. In each field survey, two to four sampling stations were set in the same transverse profile. LST rates, represented by Q_T , are estimated according to a set of equations proposed by Wang [42] as described by Eqs. 1, 2 and 3, where ΔF_i = sediment flux between two adjacent

nets (kg s⁻¹); F_{i+1} and F_{i-1} = fluxes through the upper and lower nets (kg s⁻¹), respectively; Z_{i+1} and Z_{i-1} = vertical width of the opening of the upper and lower nets (m), respectively; ΔZ_i = distance between two adjacent nets (m); l = total flux passing through all capture nets (kg h⁻¹ m⁻²); n = number of nets mounted on the trap = 10; i = identifier number of each streamer trap on the surf zone; l_i = sediment flux measured at trap array i (kg h⁻¹ m⁻²); and A_i = surf cross-sectional area between traps i and $i + 1$ (m²).

$$\Delta F_i = \left(\frac{F_{i+1} + F_{i-1}}{Z_{i+1} + Z_{i-1}} \right) \Delta Z_i \quad (1)$$

$$I = \sum_{i=1}^n F_i + \sum_{i=1}^{n-1} \Delta F_i \quad (2)$$

$$Q_T = \sum \frac{I_i + I_{i+1}}{2} A_i \quad (3)$$

The field work followed a standard procedure: (1) beach profile—profiles were taken using a Nikon Nivo 2C total station and a surveying reflection prism. Profiles were used to identify the location of sampling stations, bathymetric features, mean waterline position (mean swash zone position), breaker point depth hb (defined as the vertical distance between the seabed and the waterline in the breaking point) and beach slope, represented by the tangent of the beach inclination angle $\tan\beta$; (2) wind measurement—wind velocity and direction were measured with an anemometer, a windsock and a compass; (3) longshore current—currents were measured with a drifting buoy, made with PET bottles containing sand, a chronometer and marking stakes (Lagrangian measurement). Velocity is measured as a function of the time that the drifter takes to travel 30 m in the surf zone. This procedure is triplicated, and an average of the three values obtained is made. (4) Last is the longshore sediment transport step, in which streamer traps are used to sample sediments under longshore transport.

Sediment samples were washed with fresh water to remove the salts, dried in a stove (80–100 °C), and then, the grain size analysis was performed with a precision scale and a set of stainless steel sieves (interval $\frac{1}{4} \phi$ in the Wentworth [31] scale).

3.2 Wave data

Authorial wave data were provided by the Sistema de Monitoramento da Costa Brasileira (SiMCosta), collected with a directional waverider buoy moored adjacent to Cassino beach (32° 17' 43.03" S 52° 1' 29.95" W), 17 km apart from the coastline. Perotto [27] and Fontoura et al. [2] measured wave parameters in the breakpoint through continuous filming of wave fields with posterior laboratory analysis. All wave data were converted from its initial acquisition form to a pattern considering the transformative processes associated with wave propagation in shallower waters. The conversion was made through linear regression, using significant wave height H_S (in meters), peak wave period T_p (in seconds) and wave propagation direction D_p (in degrees) simulated in the Simulating

WAves Nearshore (SWAN) model by [30], for the isobaths of 2.5 m and 19 m. In order to obtain greater data accuracy, all of the converted wave components referred to a 4 h interval regarding the time in which field surveys were carried out. The surf zone width L_{SZ} was also estimated through linear regression using data from images obtained with the Argus video-imaging system [43, 44]. The regression was made among the L_{SZ} measured through Argus images, H_S and T_p [45]. The correlation coefficients were $r=0.95$, $r=0.98$, $r=0.96$ and $r=0.39$, respectively, for H_S , T_p , D_p and L_{SZ} (Fig. 2). Although the L_{SZ} coefficient seems low, it is significant for a 95% confidence interval with a significance level of 0.05.

3.3 LST rates

The LST rates were estimated using 4 analytical models. The model described by CERC [24] presents an equation based on the principle that LST rates are proportional to the longshore component of wave energy (Eq. 4). The LST rate Q_L corresponds to the immerse volume in $\text{m}^3 \text{s}^{-1}$, and it considers a dimensionless coefficient K —determined initially through linear regression using field data collected by Komar and Inman [8], researched later by other authors [4, 17, 18, 46–50]: gravity acceleration g (m s^{-2}), seawater density ρ_{H_2O} (kg m^{-3}), sediment particles density ρ_s (kg m^{-3}), porosity ϕ (dimensionless), H_S (m), breaker index k (in accordance with the ratio between H_S and water depth) and D_p (degrees).

$$Q_L = \frac{K \cdot (\sqrt{g})}{(16 \cdot \sqrt{k}) \cdot (\rho_s - \rho_{H_2O}) \cdot (1 - \phi) \cdot \left(H_S^{\frac{5}{2}}\right) \cdot (\sin 2 \cdot D_p)} \quad (4)$$

The model proposed by Kamphuis [25] allows to estimate LST rates Q_L as a function of wave parameters, fluid and sedimentary characteristics, and beach profiles (Eq. 5). It has similarities with Eq. 4 (i.e. dimensionless coefficient K , ρ_{H_2O} , g , H_S , D_p); however, it calculates the rates in kg s^{-1} and includes T_p (s), beach slope $\tan\beta$ (dimensionless) and median grain size D_{50} (m).

$$Q_L = K \rho_{H_2O} \left(\frac{g}{2\pi}\right)^{1.25} H_S^2 T_p^{1.5} \tan\beta^{0.75} D_{50}^{-0.25} \sin(2D_p)^{0.6} \quad (5)$$

Bayram et al. [26] define the Q_L rate ($\text{m}^3 \text{s}^{-1}$) as a product of the sediment concentration in suspension and the acting longshore current (Eq. 6). This method differs from the others mentioned before especially because it considers the mean longshore current velocity V_{LC} (m s^{-1}) in the surf zone. It is important to notice that the influence of waves, winds and tides is included in this parameter, because the total velocity is considered, not exclusively the parcel generated by the wave-induced longshore flux. Besides

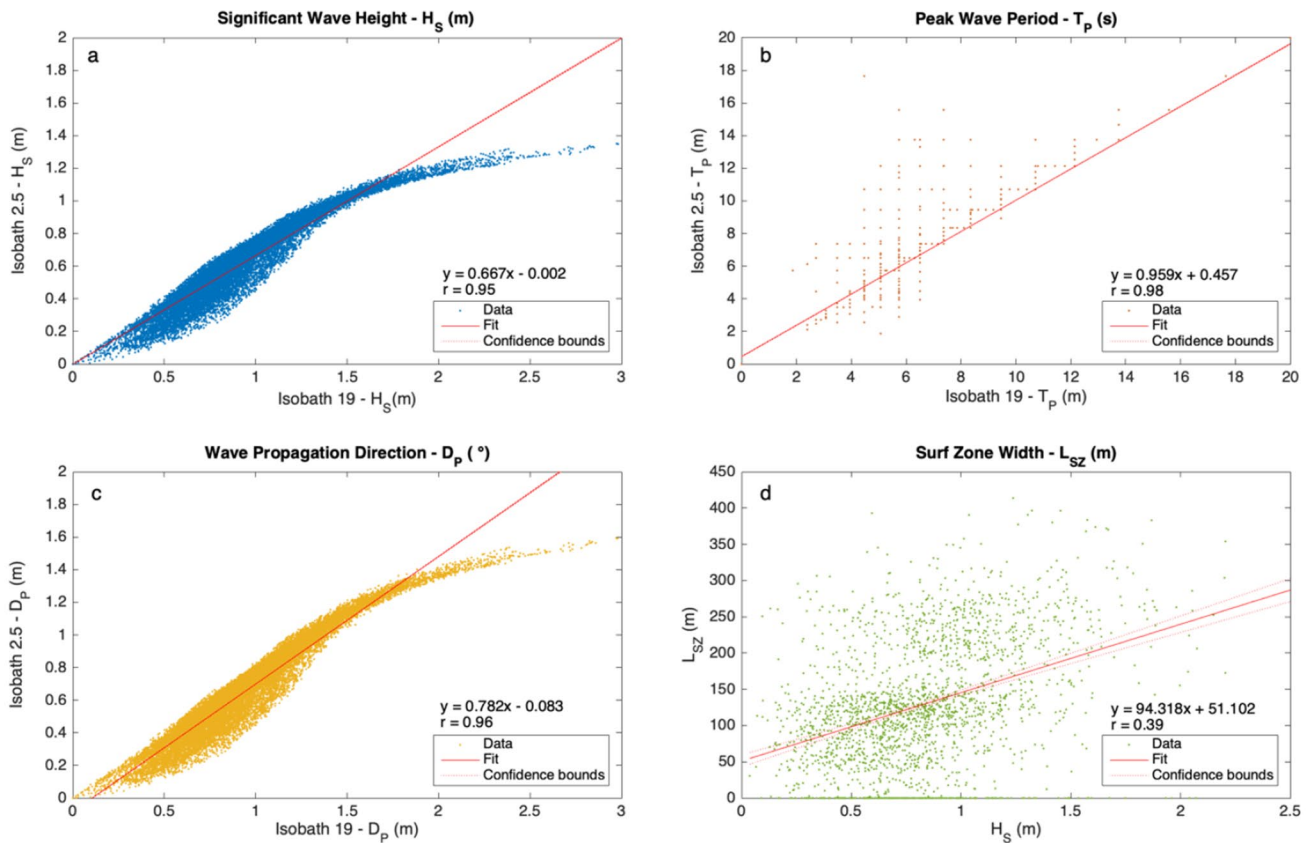


Fig. 2 Linear regression graphs referring to the relation between 19- and 2.5-m isobaths for H_S , T_p and D_p (a–c), and to the relation between L_{SZ} and H_S (d)

that, this method assumes that suspension load is the dominant transport mechanism in the surf zone because the sediment deposited on the bottom is suspended by the continuous action of waves. Hence, this model suggests a transport coefficient ϵ proportional to wave efficiency in keeping grains in suspension calculated through Eq. 7, considering the particle settling velocity W_S ($m s^{-1}$) instead of D_{50} . The wave-energy flux energy F (Eq. 8) is also considered:

$$Q_L = \frac{\epsilon}{(\rho_s - \rho_{H_2O}) \cdot (1 - \phi) \cdot g \cdot W_S} \cdot \overline{F V_{LC}} \quad (6)$$

$$\epsilon = \left(9 + 4 \cdot \frac{H_S}{W_S \cdot T_P} \right) \cdot 10^{-5} \quad (7)$$

$$F = E \cdot C_G \cdot \cos D_p \quad (8)$$

where E = wave energy ($J m^{-2}$) and C_G = wave group velocity in shallow waters ($m s^{-1}$).

Van Rijn [23] proposes to estimate the Q_L rate in $kg s^{-1}$ using a simple general equation (Eq. 9). This method is derived from a previous trial [43] with a detailed

process-based model, and in this more recent version, it is calibrated and revalidated, making Q_L a function of a mobility coefficient M obtained through Eq. 10:

$$Q_L = 0.0006 \cdot M \quad (9)$$

$$M = K_{swell} \cdot \rho_s \cdot (\tan \beta)^{0.4} \cdot (D_{50})^{-0.6} \cdot (H_S)^{2.6} \cdot V_{LC total} \quad (10)$$

$$V_{LC total} = V_{LC wave} + V_{LC wind} \quad (11)$$

$$V_{LC wave} = 0.3 \cdot (g H_S)^{0.5} \cdot \sin(2D_p) \quad (12)$$

$$V_{LC wind} = 0.01 \cdot p_1 \cdot v_1 + 0.01 \cdot p_2 \cdot v_2 \quad (13)$$

The mobility coefficient M includes beach profile effects through beach slope, represented by $\tan \beta$, and through median grain size D_{50} , aiming a wider applicability of this method when it comes to different morphodynamic stages. It also contemplates the effect of low-period swell waves ($T_p = 9–12$ s, $H_S = 0.70–2.0$ m), indirectly considering T_p , since these waves can produce

significantly larger transport rates when compared to wind waves of the same height [23].

The main equation (Eq. 10) considers the mean longshore current velocity $V_{LC\ total}$ in $m\ s^{-1}$, just like the analytical model proposed by Bayram et al. [26]. However, it allows to distinguish the velocities induced by the waves $V_{LC\ wave}$ from the tide-wind-induced velocities (Eqs. 11, 12, 13). The study area is under a microtidal regime; therefore, only the wind was considered as a influence factor over the LST, and so the tide-wind-induced velocity is represented by $V_{LC\ wind}$ (Eq. 13), in which p_1 = percentage of time with positive flow; p_2 = percentage of time with negative flow; v_1 = representative velocity in positive longshore direction due to wind ($m\ s^{-1}$); v_2 = representative velocity in negative longshore direction due to wind ($m\ s^{-1}$). $V_{LC\ WIND} = 0.1\ m\ s^{-1}$ as suggested by Van Rijn [23] for microtidal conditions.

LST rates estimation requires the awareness of many specific characteristics of the study area. Table 1 contains the values attributed to each parameter considered in the four models described above, except for the values referent specifically to the day of field surveys (i.e. waves, winds and longshore currents). It also displays information regarding data origin.

3.4 Performance verification

Analytical models were verified through different statistical methods as follows: (1) Bias—This calculation considered the resampling method through Jackknife [51], a nonparametric technique that reduces the estimator variance; (2) Root Mean Square Error (RMSE)—since LST rates extend through several orders of magnitude, logarithmic values (base 10) were considered for this statistical measure as proposed in [4]. When $RMSE = 1$, it means that the modelled values are approximately ten times bigger or smaller than the sampled ones. The remaining are (3) Scatter Index (SI); (4) Pearson Correlation; (5) Spearman's Rank Correlation; and (6) Student's t Test.

4 Results

4.1 Field surveys

This research comprehended seventeen field surveys in distinct beach locations, among the years of 2002, 2003, 2004 and 2018, under different meteoceanographic conditions. The predicted and observed results $Q_{in\ situ}$ can be seen in Fig. 3. The comparison between $Q_{in\ situ}$ and the predicted results allows to observe that the method proposed by Kamphuis [25] tends to underestimate the LST occurring in the system, representing the most unrealistic rates, varying in one order of magnitude for most of

the cases. Predictions according to the model proposed by Bayram et al. [26] also resulted in underestimated rates for most of the scenarios. When it comes to CERC [24] and Van Rijn [23], no tendencies of under- or overestimation were observed, except for high LST scenarios (20/02/2003, 05/09/2003, 12/12/2004—Sarita, 07/08/2018), in which the estimates were lower than the observed in situ.

4.2 Wave and wind data

The conversion of wave parameters resulted in significant changes in H_s and D_p , but not in T_p , which was almost constant for all the scenarios. Waves reduced around 33.9% of their original height, and the direction changed approximately 21.9%, also with a reduction trend from the angle found at the 19-m isobath. The final converted values are in Table 2.

Multiple linear regression was applied aiming to identify the meteoceanographic agents with more influence over longshore currents and LST rates. The statistical tests were reproduced using different combinations between wind and wave variables (Table 3). It is important to notice that some of the displayed regressions consider wind direction instead of velocity, as seen in others, because only the best multilinear responses are shown in this table. Waves have more influence over the LST, for all parameters: LC velocity ($r = 0.73$), LC direction ($r = 0.96$) and LST rate ($r = 0.89$). Wind is only statistically significant over LC velocity ($r = 0.70$) and direction ($r = 0.74$). Although waves are more influent, when wave and wind components are combined as predictor variables, at least 95% of the LST is explained statistically, for all components.

4.3 Analytical modelling

The statistical results (Table 4) demonstrated that the model proposed by Van Rijn [23] is the most applicable to estimate LST rates in the southern region of Brazil. Van Rijn [23] was the only method that showed good results for all verification tests applied, being statistically significant in confidence levels of 95% ($\alpha = 0.05$) and 99% ($\alpha = 0.01$), for both correlations (Pearson and Spearman). It is the only model in which t -test has enough evidence to support that the predicted rates correspond to the observed values, and it is also the model with the lowest SI and RMSE.

Although CERC [24] has a t value that rejects the hypothesis that the predicted rates are similar to the observed ones, the correlation coefficients r and r_s are significant for the confidence intervals of 95% ($\alpha = 0.05$) and 99% ($\alpha = 0.01$). Moreover, this model results showed the lowest bias and low values of SI and RMSE. In this way, CERC [24] was considered the second most adequate method for the estimation of longshore transport rates

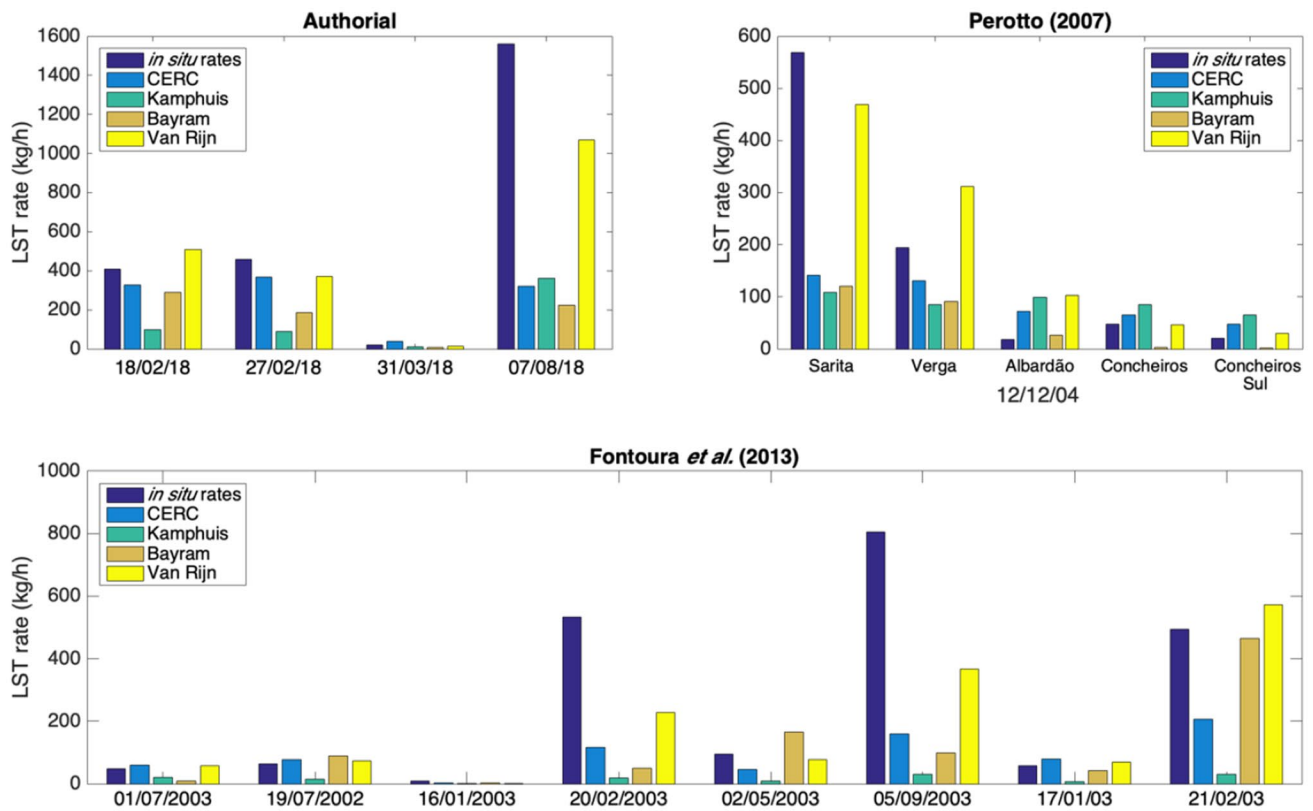


Fig. 3 Bars for LST rates comparing the predicted and observed data for each author. Notice that for Perotto [21], all field surveys occurred in the same date, and Fontoura et al. [2] rates are not

arranged chronologically because they are disposed according to their sampling sites, as displayed in Table 2

in the study area. Neither Kamphuis [25] nor Bayram et al. [26] performed adequately for the region under study.

5 Discussion

5.1 Wave and wind data

Waves have more influence over the LST overall, and this can be clearly seen through the correlation coefficients, specially for Q_T , for which the wind itself is not statistically significant. Although waves presented the highest correlation coefficients for all the variables under consideration, their influence can be altered by wind interference, as seen specially during field surveys. That means they are statistically sufficient when isolated to explain entirely the LST mechanism, but not enough to describe real scenarios. Wind parameters are relevant to the direction and velocity of longshore currents. Thus, the combination of wave and wind components as predictor variables explained more than 95% of the three properties evaluated. This demonstrates that LST is a direct reflex of the concomitant action of both agents, in a way longshore currents are

set up, predominantly, by the characteristics of its generation wave, and the wind corroborates with the dynamics involved in the flux, influencing, hence, the amount of sediment mass being transported and in the resulting LST.

Beyond the statistics, the influence of winds was observed during the current author’s field surveys: in 31 March 2018, the opposite incidence directions between the waves and the wind resulted in a low longshore sediment transport (forces were almost cancelling each other), and in 7 August 2018, the action of both components coming from the same quadrant resulted in an intensified LST rate, the highest value among all the period under investigation. In that way, it can be affirmed that the wind has potential to reduce or increase wave action over LC generation and, consequently, over LST, except when its intensity is too low or absent.

Besides being the most accurate model overall, Van Rijn [23] performed better for the authorial measurements than for the other datasets as seen in Fig. 3. It is supposed that the differences between wave data acquirement influenced the simulated rates. Thus, predictions were more accurate when wave parameters were sampled with SiMCoSta buoy and later converted, rather

Table 2 Meteoenographic conditions for each field survey. The sampled data are used as input to the analytical models and as a source to the performance verification of the models

Author	Date	Location	Wind			Waves			LC		LST
			V_{WIND} (m s ⁻¹)	D_{WIND} (°)	H_S (m)	T_p (s)	D_p (°)	L_{SZ} (m)	V_{CL} (m s ⁻¹)	Direction	
Fontoura et al. [2]	01/07/2003	Cassino beach—EMA	2.0	307	0.57	14	117	104.86	0.14	NE-SW	48.52
	19/07/2002	Cassino beach—terminal	4.5	2	0.59	11.2	132	106.75	0.41	NE-SW	64.54
	16/01/2003		6.0	32	0.15	3.0	102	65.25	0.31	NE-SW	9.34
	20/02/2003		3.0	207	0.78	9.4	137	124.67	0.10	SW-NE	533.53
	02/05/2003	West jetty root	7.0	207	0.72	8.5	167	119.01	0.28	SW-NE	94.41
Perotto [21] ^a	05/09/2003	Mar Grosso beach—east jetty root	3.6	327	0.97	11.6	137	142.59	0.36	SW-NE	805.27
	17/01/2003	Mar Grosso beach—3 km from east jetty	6.0	32	0.68	7.0	117	115.24	0.37	NE-SW	58.41
	21/02/2003	Mar Grosso beach—12 km from east jetty	7.0	207	1.26	8.6	147	169.94	0.70	NE-SW	494.94
	12/12/2004	Sarita	-	-	0.90	9.0	40	135.84	0.32	NE-SW	568.85
		Verga	-	-	0.87	7.0	37.5	132.70	0.21	NE-SW	194.11
Author's measurement		Albardão	-	-	0.56	12.0	40	104.39	0.27	NE-SW	18.28
		Concheiros	-	-	0.53	12.0	37.5	101.24	0.41	NE-SW	47.12
		Concheiros Sul	-	-	0.46	12.0	60	94.95	0.46	NE-SW	20.09
	18/02/2018	Cassino beach—EMA	3.88	63.6	0.74	6.64	74.01	155.79	0.46	NE-SW	409.97
	27/02/2018		5.30	105	0.60	10.55	112.92	136.70	0.39	NE-SW	459.42
	31/03/2018		180	0.50	6.93	93.17	122.55	0.15*	SW-NE	19.91	
	07/08/2018		30	0.76	11.44	80.46	159.33	0.52	NE-SW	1561.11	

^aPerotto [21] did not sample wind data during field surveys

Table 3 Multiple linear regression coefficients relating LC velocity, LC direction and LST rates with wave and wind parameters

Dependent variable	Predictor variable	<i>r</i>	<i>R</i> ²	Significance	CI=95%
Longshore current— <i>V</i> _{LC} (m s ⁻¹)	Wave— <i>H</i> _s , <i>T</i> _p , <i>D</i> _p	0.73	0.53	Significant	
	Wind—velocity and direction	0.70	0.49	Significant	
	Wave— <i>H</i> _s , <i>T</i> _p	0.99	0.98	Significant	
	Wind—velocity				
Longshore current—direction (°)	Wave— <i>H</i> _s , <i>T</i> _p , <i>D</i> _p	0.84	0.71	Significant	
	Wind—velocity and direction	0.74	0.54	Significant	
	Wave— <i>H</i> _s , <i>T</i> _p	0.99	0.97	Significant	
	Wind—direction				
LST rate— <i>Q</i> _T (kg h ⁻¹)	Wave— <i>H</i> _s , <i>T</i> _p , <i>D</i> _p	1.00	1.00	Significant	
	Wind—velocity				
	Wave— <i>H</i> _s , <i>T</i> _p , <i>D</i> _p	0.89	0.79	Significant	
	Wind—velocity and direction	0.40	0.16	Not significant	
	Wave— <i>H</i> _s , <i>T</i> _p	0.96	0.93	Significant	
	Wind—velocity				
	Wave— <i>H</i> _s , <i>D</i> _p	0.95	0.91	Significant	
	Wind—velocity				

Table 4 Statistical parameters referring to the analytical models performances

Analytical model	Bias	RMSE	SI	Pearson correlation		t test		Spearman's rank correlation	
				<i>r</i> _{95%}	<i>R</i> ²	<i>t</i> _{95%} ^a	Result	<i>r</i> _s 95%	<i>P</i> value
CERC [24]	0.03	0.33	0.0010	0.71	0.50	2.25	1—hypothesis rejected	0.81	0.0001
Kamphuis [25]	-0.35	1.46	0.0046	0.76	0.58	2.99	1—hypothesis rejected	0.44	0.0762
Bayram et al. [26]	0.09	1.08	0.0034	0.49	0.25	2.37	1—hypothesis rejected	0.80	0.0002
Van Rijn [23]	-0.05	0.18	0.0006	0.93	0.86	1.40	0—hypothesis not rejected	0.86	0

^aHypothesis test based on Student's t-distribution, with 16 freedom degrees and a critical value *t*_{cr}=2.120, for a significance level *α*=0.05. Null hypothesis *H*₀—*μ*_{MODEL}=*μ*_{in situ}; alternative hypothesis *H*₁—*μ*_{MODEL}≠*μ*_{in situ}

than by observations and filming in the beach field work as made by Perotto [27] and Fontoura et al. [2]. Moreover, the conversion of wave parameters was relevant for this study considering that longshore currents are mostly influenced by nearshore breaking waves. During wave propagation from deep waters to 15-m and 18-m isobaths, wave transformation processes start, and as they gradually approach shallower waters, *H*_s and *D*_p change their values as an adjustment caused by energy conservation through these processes (i.e. refraction, diffraction and shoaling). *D*_p is modified in a way the crests tend to become parallel to the bathymetric contours. Therefore, NE and SW waves gradually disappear, focusing their directions on E and SE quadrants in the southern coast of Rio Grande do Sul [2], quadrants which are associated with the most energetic scenarios, and so the highest LST rates. The alterations occurred in *D*_p are mainly attributed to refraction, and the variations occurred in *H*_s represent, partially, the redistribution of the energy flux seeking its conservation.

Furthermore, wave celerity and length diminish progressively towards the coast at the same time wave height tends to increase (these values will keep changing until the wave breaks, dissipating its energy), and the period remains nearly constant [3].

5.2 LST rates

The predictability skill of each analytical model depends on the parameters involved in the equations for the calculation of LST rates. Accordingly, different analytical formulae resulted in distinct values for the same meteoceanographic conditions.

Van Rijn [23] was proven to be applicable in sandy and mixed beach systems, given its good performance among all the different beaches studied herein. Notwithstanding, the models elected as most adequate tend to underestimate the observed rates during high-energy scenarios, like the other two tested. The underrates can

be partially attributed to the inaccuracy of the coefficients involved in the equations, as discussed by Van Rijn [23] through the suggestion of a new formula with calibrated factors, and also related to the lack of sampled data during high-energy events, since these values are usually not considered in model validation and calibration, and it is when the highest LST rates occur [2]. Moreover, wind influence is only considered in Van Rijn [23] and Bayram et al. [26] calculations through the LC velocity. Considering the wind's potential to alter longshore currents, and so the LST, as seen in the multilinear regressions (Table 3), the underestimates associated with high-energy conditions may be attributed to the negligence of relevant wind components in the analytical models. This is exemplified by 07 August 2018 scenario, date in which the biggest LST value was observed, but none of the models were able to fully predict it, and the wind velocity was expressive (around 7 m s^{-1} with 8 m s^{-1} gusts). Bayram et al. [26] contemplate wind effects, but it does not consider beach slope and D_{50} (sediment size is indirectly considered through W_s). Given these two parameters are very relevant for LST, jointly with wave properties [4, 14, 23], and considering that W_s does not change the net longshore transport, as computed by [14, 26], predictions presented many inaccuracies. In that way, further investigations are required to validate a model with a more accurate wind effect, and to calibrate the Van Rijn [23] equation, increasing, possibly, its accuracy.

The tendencies observed presented a positive proportionality between H_s , beach slope and LST rates, and a negative proportion with D_{50} [4, 14, 23, 26], likewise the trends occurring in the results herein. Albardão and Concheiros Sul scenarios exemplify the effect of D_{50} , in which the suspended load transport is diminished because grain size increases. D_{50} , $\tan \beta$, H_s and D_p at the breaker line are the key parameters for predicting LST rates according to [23]. Waves are also the most influent agent in the current study; however, the most significant regression responses are associated with T_p (influencing wave type and energy), instead of D_p as postulated in [23], although wave propagation direction was still very significant in this research. This may be related to the importance of swell effect, computed indirectly through peak wave period, and highlighted by the good performance of Van Rijn [23].

Bergillos et al. [13] evaluated the performance of empirical equations (i.e. Inman and Bagnold [7], CERC [24], Kamphuis [25] and Van Rijn [23]) through RMSE and through a ratio between the predicted and the observed rates. Their results pointed that all four equations tend to overestimate LST rates when D_{50} is based on the sandy fraction of bimodal beaches, but Van Rijn [23] is still the most accurate model overall. When gravel is considered, [23]

efficiency is improved and the model presents the lowest RMSE associated, highlighting, once more, that grain size is a key parameter for estimating LST rates.

Concheiros Beach has a bimodal sediment distribution ($D_{50}=0.2102$ and $D_{50}=0.707$ mm according to [28]), and like Bergillos et al. [13], the most accurate LST rates were found in this study when the gravel fraction was under consideration. Therefore, the agreement with [13] results sustain, once again, Van Rijn [23] as the most adequate model for the southern coast of RS, since the best model elected by them is the same found herein, and they also looked for a model applicable in sandy, mixed and shingle beaches. The current study area is predominantly composed of fine sandy beaches, but the southernmost stretches are composed of coarse sand and bioterritic gravel (i.e. Sarita, Albardão, Concheiros). Thus, Van Rijn [23] applicability is proven to be efficient on coasts with a variable grain composition.

LST behavioural response will be different for each beach morphodynamic stage and meteoceanographic component in intensity, in agreement proportion, and in different time and space scales (may these components be related to wind, waves, tide, sedimentology, geomorphology and/or others). Furthermore, the contribution of each property able to influence the LST mechanism is not fully understood, and their weight factors still need to be investigated, specially when it concerns new tests with datasets around different world regions [12–14, 16, 20, 21, 52–55]. Therefrom, studies referring to each specific study area may be conducted, considering the main characteristics of the beach system under study, so the most applicable methodology can be chosen and the prediction of LST rates can be more accurate.

6 Conclusions

The observed LST rates demonstrated that this phenomenon varies as a function of daily meteoceanographic conditions, specially referring to wave and wind components. The predictability skill of each model is dependent on the parameters considered in its main equation, and the factors of influence each one has over the LST. Therefore, the results obtained through distinct analytical formulae were discrepant for the same beach under the same meteoceanographic scenario.

Wave parameters, median grain size and beach slope were proven to strongly influence longshore sediment transport, as found by previous studies, corresponding to the choice of best model overall. During high-energy scenarios, predictions were underestimated for all analytical models considered herein. Van Rijn [23] results were slightly closer to the observed rates, when compared to

the others, and this may be attributed to its inclusion of swell factor and wind-induced longshore velocity, demonstrating the importance of wind in LST predictions.

Results herein can be compared with available literature in other regions around the world, but it is important to notice that LST behavioural response and model's effectiveness will be different for each specific study area, especially in what concerns the beach morphodynamic stage and proportionality feedback between longshore transport and system component. Hence, the method prediction accuracy depends greatly on the suitability of the dataset with respect to the analytical model being used.

Overall, this study demonstrates that every effort towards the assessment of LST is still needed since it has been studied for many decades by scientists from all around the world, and it is not fully comprehended yet, still presenting inaccuracies.

Acknowledgements This study had the support of Laboratório de Oceanografia Geológica—LOG—at Universidade Federal do Rio Grande—FURG. The authors also acknowledge Dr. José A. S. Fontoura for providing all the information regarding field surveys with streamer traps, besides the equipment itself, which were indispensable for obtaining the data used herein.

Author contributions All authors contributed to the study conception and design. Material preparation, data collection and analysis were performed by Gabrielle Pereira Quadrado and Elaine Siqueira Goulart. The first draft of the manuscript was written by Gabrielle Pereira Quadrado, and both authors commented on previous versions of the manuscript. All authors read and approved the final manuscript.

Availability of data and material Most of the data used herein were collected and analyzed by the authors (these are specified along the manuscript), although wave data were provided by the Sistema de Monitoramento da Costa Brasileira—SiMCosta, and some predictive scenarios were simulated using the datasets of Perotto [27] and Fontoura et al. [2].

Code availability Analytical models, statistical tests and graphs were computed through MATLAB. The map referring to the study area was produced in QGIS3.4.

Compliance with ethical standards

Conflicts of interest The authors declare that they have no conflict of interest.

References

1. Wright LD, Short AD (1984) Morphodynamic variability of surf zones and beaches: a synthesis. *Mar Geol* 56(1–4):93–118
2. Fontoura JAS, Almeida LE, Calliari LJ, Cavalcanti AM, Moller OJ, Romeu MAR, Christófaro BR (2013) Coastal hydrodynamics and longshore transport of sand on Cassino Beach and on Mar Grosso Beach, Southern Brazil. *J Coast Res Coconut Creek* 289:855–869
3. Komar PD (1998) Beach processes and sedimentation, 2nd edn. Prentice Hall, Upper Saddle River
4. Mil-Homens J, Ranasinghe R, van de Thiel Vries JSM, Stive MJF (2013) Re-evaluation and improvement of three commonly used bulk longshore sediment transport formulas. *Coast Eng* 75:29–39
5. Sedrati M, Anthony EJ (2007) Storm-generated morphological change and longshore sand transport in the intertidal zone of a multi-barred macrotidal beach. *Mar Geol* 244:201–229
6. Wyrski VK (1953) The balance of littoral transport in the surf zone. *Deutsche Hydrographische Zeitschrift* 6(2):65–76
7. Inman DL, Bagnold RA (1963) Littoral processes. In: Hill MN (ed) *The sea 3: the earth beneath the sea history*. Interscience, New York, pp 529–533
8. Komar PD, Inman DL (1970) Longshore sand transport on beaches. *J Geophys Res* 75(3):5914–5927
9. Kraus NC (1987) Application of portable traps for obtaining point measurements of sediment transport rates in the surf zone. *J Coast Res* 3(2):139–152
10. Camenen B, Larroude P (2003) Comparison of sediment transport formulae for the coastal environment. *Coast Eng* 48(2):111–132
11. Hanson H, Kraus NC (2011) Long-term evolution of a long-term evolution model. *J Coast Res* 59(Special Issue):118–129
12. Fernández SF, Baptista P, Martins VA, Silva PA, Abreu T, Pais-Barbosa J, Bernardes C, Miranda P, Rocha MVL, Santos F, Bernabeu A, Rey D (2016) Longshore transport estimation on Ofir Beach in Northwest Portugal: sand-tracer. *J Waterw Port Coast Ocean Eng* 142(2):1–14
13. Bergillos RJ, Ortega-Sánchez M, Masselink G, Losada MA (2016) Morpho-sedimentary dynamics of a microtidal mixed sand and gravel beach, Playa Granada, southern Spain. *Mar Geol* 379:28–38
14. Noujas V, Kankara RS, Rasheed K (2018) Estimation of longshore sediment transport rate for a typical pocket beach along west coast of India. *Mar Geod* 41(2):201–216
15. Khalfani D, Boutiba M (2019) Longshore sediment transport rate estimation near harbor under low and high wave-energy conditions: fluorescent tracers experiment. *J Waterw Port Coast Ocean Eng* 145(4):04019015
16. Bergillos RJ, Rodríguez-Delgado C, Ortega-Sánchez M (2017) Advances in management tools for modeling artificial nourishments in mixed beaches. *J Mar Syst* 172:1–13
17. Mason T, Voulgaris G, Simmonds DJ, Collins MB (1997) Hydrodynamics and sediment transport on composite (mixed sand/shingle) and sand beaches: a comparison. In: *Proceedings of the 3rd coastal dynamics*. ASCE, pp 48–57
18. Buscombe D, Masselink G (2006) Concepts in gravel beach dynamics. *Earth Sci Rev* 79:33–52
19. Masselink G, McCall RT, Poate T, Van Geer P (2014) Modelling storm response on gravel beaches using XBeach-G. In: *Proceedings of the institution of civil engineers-maritime engineering*. Thomas Telford Ltd., pp 173–191
20. Tomasicchio GR, D'Alessandro F, Barbaro G, Maiara G (2013) General longshore transport model. *Coast Eng* 71(1):28–36
21. Tomasicchio GR, D'Alessandro F, Barbaro G, Musci E, De Giosa TM (2015) Longshore transport at shingle beaches: an independent verification of the general model. *Coast Eng* 104:69–75
22. Van Rijn LC (2002) Longshore sand transport. In: *28th international conference on coastal engineering (ICCE)* Cardiff, UK, pp 2439–2451
23. Van Rijn LC (2014) A simple general expression for longshore transport of sand, gravel and shingle. *Coast Eng* 90:23–33
24. U.S. Army Corps of Engineers (USACE) (1984) Shore protection manual. Coastal Engineering Research Center (CERC), US Army

- Corps of Engineers Research and Development Center, Coastal and Hydraulics Laboratory, v. 2, Vicksburg, Mississippi.
25. Kamphuis JW (1991) Alongshore sediment transport rate. *J Waterw Port Coast Ocean Eng* 117(6):624–640
 26. Bayram A, Larson M, Hanson H (2007) A new formula for the total longshore sediment transport rate. *Coast Eng* 54:700–710
 27. Perotto H (2007) Influência do transporte sedimentar longitudinal nas variações da linha de costa no litoral sul do Rio Grande do Sul. Monograph, Federal University of Rio Grande – FURG.
 28. Calliari LJ, Klein AHF, Barros FCR (1996) Beach differentiation along the Rio Grande do Sul coastline (Southern Brazil). *Rev Chil de Hist Nat* 69:485–493
 29. Figueiredo SA, Calliari LJ (2006) Sedimentologia e suas Implicações na Morfodinâmica das Praias Adjacentes às Desembocaduras da Linha de Costa do Rio Grande do Sul. *Gravel* 4:73–87
 30. Goulart ES (2014) Variabilidade morfodinâmica temporal e eventos de inundação em um sistema praias com múltiplos bancos. Thesis, Doctoral dissertation. Federal University of Rio Grande – FURG
 31. Guedes RMC, Calliari LJ, Pereira PS (2009) Morfodinâmica da praia e zona de arrebatamento do Cassino, RS através de técnicas de vídeo imageamento e perfis de praia. *Pesquisas em Geociências* 36(2):165–180
 32. Calliari LJ, Klein AHF (1993) Características Morfodinâmicas e Sedimentológicas das Praias Oceânicas Entre Rio Grande e Chuí, RS. *Pesquisas em Geociências* 20:48–56
 33. Espírito Santo RM (2007) Variabilidade morfodinâmica entre as regiões da Querência e do Navio Altair na Praia do Cassino, RS, Brasil. Dissertação (Mestrado em Oceanografia Química, Física e Geológica)—Universidade Federal do Rio Grande—FURG, Rio Grande.
 34. Martins LR (1967) Aspectos deposicionais e texturais dos sedimentos praias e eólicos da Planície Costeira do Rio Grande do Sul. Publicação Especial da Escola de Geologia, Universidade Federal do Rio Grande do Sul—UFRGS, Porto Alegre
 35. Bessler KE, Rodrigues LC (2007) The polymorphs of calcium carbonate—an easy synthesis of aragonite. *Química Nova* 31(1):178–180
 36. Tomazelli LJ, Villwock JA (1992) Algumas Considerações sobre o Ambiente Praial e a Deriva Litorânea de Sedimentos ao longo do Litoral Norte do Rio Grande do Sul, Brasil. *Pesquisas em Geociências* 19:1–26
 37. Parise CK, Calliari LJ, Krusche N (2009) Extreme storm surges in the South of Brazil: atmospheric conditions and shore erosion. *Braz J Oceanogr* 57(3):175–188
 38. Reboita MS, Krusche N, Piccoli HC (2006) Climate variability in Rio Grande, RS, Brazil: a quantitative analysis of contributions due to atmospheric systems. *Rev Bras Meteorol* 21(2):256–270
 39. Williams JJ, Esteves LS (2006) Predicting shoreline response to changes in longshore sediment transport for the Rio Grande do Sul coastline. *Braz J Aquat Sci Technol* 10(1):1–9
 40. Esteves LS, Williams JJ, Dillenburg SR (2006) Seasonal and interannual influences of the patterns of shoreline changes in Rio Grande do Sul, Southern Brazil. *J Coast Res* 22(5):1076–1093
 41. Albuquerque MG, Fontoura JAS, Calliari LJ, Serpa CG, Falcão TO (2008) Caracterização do fluxo sedimentar na zona de surfe de praias de micro e meso marés – aplicação a praia do Cassino (RS) e praia do Futuro (CE). In: *Anais do III Seminário e Workshop em Engenharia Oceânica (SEMENGO'2008)*. Rio Grande, RS, Brasil: Universidade Federal do Rio Grande (FURG)
 42. Wang P, Kraus NC, Davis RA Jr (1998) Total longshore sediment transport rate in the surf zone: field measurements and empirical predictions. *J Coast Res* 14(1):269–282
 43. Holman RA, Stanley J (2007) The history and technical capabilities of Argus. *Coast Eng* 54:477–491
 44. Guedes RMC (2008) Utilização de métodos diretos e vídeo-imagens ARGUS na caracterização morfodinâmica da zona de arrebatamento da Praia do Cassino, RS. Dissertação (Mestrado em Oceanografia Física, Química e Geológica) – Universidade Federal do Rio Grande – FURG, Rio Grande
 45. Ribeiro KG, Goulart ES (2017) Identificação manual e semiautomática da zona de arrebatamento em vídeo imagens. *Anais do Congresso da ABEQUA 2017—Mudanças Climáticas no Passado e no Presente: conhecer para entender as consequências no future*. Bertioga, p 3
 46. Kamphuis JW, Readshaw JS (1978) A model study of alongshore sediment transport rate. In: *Proceedings of 16th international conference on coastal engineering*. ASCE Press, New York, pp 1656–1674
 47. Bailard JA (1981) An energetics total load sediment transport model for a plane sloping beach. *J Geophys Res* 86(C11):10938
 48. Leont'yev IO (1989) Dynamics of surf zone. Shirshov Institute of Oceanology USSR Science Academy, Moscow
 49. Dell Valle R, Medina R, Losada MA (1993) Dependence of coefficient K on grain size. *J Waterw Port Coast Ocean Eng* 119:568–574
 50. Dean RG, Dalrymple RA (2002) *Coastal processes with engineering applications*. Cambridge University Press, Cambridge
 51. Quenouille MH (1949) Problems in plane sampling. *Ann Math Stat* 20(3):355–375
 52. Jackson NL, Nordstrom KF, Farrel EJ (2017) Longshore sediment transport and foreshore change in the swash zone of an estuarine beach. *Mar Geol* 386:88–97
 53. Sheela LN, Sundar V, Kurian NP (2015) Longshore sediment transport along the coast of Kerala in Southwest India. *Procedia Eng* 116:40–46
 54. Sadeghifar T, Barati R (2018) Prediction of longshore sediment transport rate using soft computing techniques and comparison with semi-empirical formulas. In: *International Energy and Environment. Chapter 8 Progress in River Engineering & Hydraulic Structures*, vol 2, pp 151–174
 55. Moghaddam EI, Hakimzadeh H (2019) Wave climate variability and longshore sediment transport evaluation along Ramin Harbor, Southeast Coast of Iran. *Int J Coast Offshore Eng* 2(3):53–62
 56. Wentworth CK (1922) A scale of grade and class terms for clastic sediments. *J Geol* 30:377–392

Publisher's Note Springer Nature remains neutral with regard to jurisdictional claims in published maps and institutional affiliations.